Proceedings of IMECE2005
2005 ASME International Mechanical Engineering Congress and Exposition
November 5-11, 2005, Orlando, Florida USA

IMECE2005-82786

CONCEPTS FOR POWER AND ENERGY ANALYSIS IN NASTIC STRUCTURES

Dr. Victor Giurgiutiu
Department of Mechanical Engineering
Laboratory for Active Materials and Smart Structures
University of South Carolina
Columbia, South Carolina
Email: giurgiut@engr.sc.edu

Luke Matthews
Department of Mechanical Engineering
Laboratory for Active Materials and Smart Structures
University of South Carolina
Columbia, South Carolina
Email: matthela@engr.sc.edu

Dr. Donald J. Leo
Department of Mechanical Engineering
Center for Intelligent Materials and Smart Systems
Virginia Tech
Blacksburg, Virginia 24061
Email: donleo@vt.edu

Vishnu Baba Sundaresan
Department of Mechanical Engineering
Center for Intelligent Materials and Smart Systems
Virginia Tech
Blacksburg, Virginia 24061
Email: vishnubaba@vt.edu

ABSTRACT

Nastic structures are potentially high-energy density smart materials that will be capable of achieving controllable deformation and shape change due to internal microactuation that functions on principles found in the biological process of nastic motion. In plants, nastic motion is accomplished through osmotic pressure changes causing a respective increase or decrease in cell volume, thereby causing net movement. In nastic structures, osmotic pressure is increased by moving fluid from low concentration to high concentration areas by means of active transport, powered by adenosine triphosphate (ATP) hydrolysis. Power analysis involves calculating possible ranges of actuation as a result of interior pressure exchanges and hydraulic flux rates which will determine the speed of actuation. Because pressure inside the actuating cylinder is uniform, the cylinder undergoes deformation in all the three dimensions. Predicting the work-energy balance involves considering the factors that determine the total volumetric change, including cylinder wall expansion, surface bulging and stretching, and outside forces that oppose the actuation. The hydraulic flux rates determine both the force magnitude and the actuation speed. Energy analysis considers the pressure variation range needed to accomplish the desired actuation deflection, and the energy required for active transport mechanisms to move the volume of fluid into the nastic actuator. Nonlinear effects are present, as the pressure inside the actuation cylinder increases, it takes more energy for active transport to continue moving fluid into it. The chemical reaction of ATP hydrolysis supplies the energy for active transport, which is related to the ratio of the reactants, to the products, as well as to the pH level. As the pH lowers, more energy is released through ATP hydrolysis. Therefore, as pH decreases, ATP Hydrolysis releases more energy, enabling active transport to move more fluid into the actuation cylinder, thereby increasing the internal osmotic pressure and causing material deformation work and actuation.

Keywords Nastic Structures, Smart Materials, Microactuation, ATP Hydrolysis, Controllable Deformation, Active Transport

INTRODUCTION

In the plant kingdom, plants are capable of localized movement due to a biological process called nastic motion in specialized motor cells. This occurs when biochemical reactions cause water to flow into or out of the motor cells, causing cellular volume change and overall tissue deformation. When the plant tissue undergoes non-uniform elongation from increased osmotic pressure or shrinkage from a decrease in pressure, the tissue will have bending deflection.

Biological nastic motion is what causes plants to angle their stems so that their leaves face light sources and flower pedals to open. Plant motor cells can be considered the muscles

of biological systems, and the process of nastic motion the driving force.

Synthetic nastic structures are materials that are capable of performing mechanical work in the form of physical shape change using the same biological processes utilized in the plant kingdom. Shape change is caused by hydraulic actuators that are modeled after the motor cells that expand and contract in plant tissues.

Because tissue movement in plants is a result of volumetric change in motor cells due to varying osmotic pressure, the range of movement is limited by the availability of fluid and the ability of the plant to transport fluid into or out of the motor cells. Design of control mechanisms of shape change in synthetic nastic structures function on these same limitations.

Analysis of osmotic pressure change on physical expansion and the factors that affect active transport of the fluid reveal ways that synthetic nastic structure deformation is best controlled. Examining the conditions that modify the range of energy released by ATP hydrolysis and used by active transport in the system shows how chemical factors such as pH and mass-action ratios of products and reactants in hydrolysis limit the possible amount of transported fluid, therefore controlling the osmotic pressure variation and volumetric deformation, and overall shape change.

NASTIC MOVEMENT IN BIOLOGICAL SYSTEMS

Most plants are capable of a limited range of gradual motion due to non-uniform swelling from osmotic pressure change. Gradual motion causes plants to angle their leaves towards light, or open their flower pedals from a closed bud. Plants are mostly sedentary, but rapid movement is essential for certain species. Quick motion aids plants in reproduction when seeds and pollen are expelled, as well as in defense, which occurs in organisms such as *Mimosa sensitiva*, that close their leaves into a tight cluster when stimulated by touch or heat [1]. Perhaps the best example of rapid nastic movement in plants is *Dionaea muscipula*, the Venus flytrap, whose jaws can snap closed in 100 ms when stimulated by prey due to the high osmotic pressure flux rate.

Typical plant tissue that undergoes nastic motion usually moves in rectolinear translation at a gradual pace over the course of several minutes. However, plants such as the *Mimosa sensitiva* and *Dionaea muscupula* move at a much faster rate about an axis. The specialized leaves rotate about a fixed node on the plant stem, or “jaw” hinge in the case of the Venus flytrap. At the center of rotation, motor cells are higher in number and condensed near the axis, but motor cells are also found throughout the leaves. These motor cells are more sparsely distributed, and also expand and contract during motion to bend the leaf in a slightly concave shape to increase angular velocity and acceleration [1].

Modeling the biochemical reactions that cause rapid hydraulic actuation plants reveals how an actuation system can be created synthetically and accurately controlled.

BIOCHEMISTRY OF NASTIC MOVEMENT

Motor cells expand in size when fluid pushes outward on the cell membrane when osmotic pressure is increased, and decrease in size when this pressure is reduced, removing the outward push on the membrane. Pressure is reduced naturally by osmotic diffusion, when water passes through the membrane channels from the fluid pressure pushing it out into a lower pressure area.

Cell membranes are made from a bilayer of phospholipids molecules. Each molecule has a hydrophilic phosphate head section and a hydrophobic tail made of lipids. The hydrophobic tails are aligned so that they face inward and the hydrophilic heads face outwards, creating a solid double layer of phospholipids.

Because of the hydrophobic interior, water cannot pass directly through the membrane. Instead, protein transport mechanisms embedded in the membrane act as a channel to allow the fluid molecules to pass through them. In a process called active transport, embedded membrane transport proteins move fluid against an osmotic pressure gradient, from a relatively low pressure reservoir to a higher pressure cell interior.

Transport proteins are like gates that are normally closed, but can be opened to initiate active transport when they are activated by a proton stimulant. The energy to activate the transport proteins comes from protons released in the reaction Adenosine triphosphate (ATP) hydrolysis and increases as the difference in the osmotic pressure gradient rises. Flux rates and the quantity of fluid actively diffused in active transport vary in organic cells depending on the difference in interior concentration of the solute and the outer concentration. Other chemicals in the medium such as sodium, potassium, and chloride also affect active transport by creating a transmembrane electric potential, potentially either inhibiting molecular transport or decreasing the energy required to power the transport proteins, increasing flux rates. In biological systems, the concentration of potassium and sodium are often determinant of the efficiency and speed of active transport mechanisms, and in cases of extreme concentrations, the proteins can be inhibited to the point of endangering the well-being of the cell [2].

ATP hydrolysis breaks down ATP molecules into adenosine diphosphate (ADP) and a PO_4^{2-} phosphate while releasing energy. It is one of the most common chemical reactions in biological systems, and also one of the most exergonic. ATP is kinetically stable around pH 7, with a high level of activation energy, thereby requiring an enzyme catalyst to initiate hydrolysis. However, when the pH level of an ATP solution is lower, the activation energy also decreases, increasing spontaneity of the reaction, making rapid hydrolysis possible without requiring enzymatic activity[5]. The amount of free energy released by ATP hydrolysis is also a result of the concentrations of ATP and the products of the reaction, ADP and PO_4^{2-}. The proportion of reactant to products is the mass-action ratio, which varies in organic systems when ATP is generated through glycolysis or ADP is converted back into ATP [6]. The mass action ratio is a limiting factor in the free energy of ATP hydrolysis in addition to pH levels of the solution.

SYNTHETIC NASTIC STRUCTURES

Motor cells in plants that undergo nastic motion can be viewed as naturally occurring hydraulic actuators. When the plant is stimulated by the presence of certain chemicals or a change in temperature, pressure, or light absorption, the cells that sense the stimulant trigger the biological processes that cause nastic motion. The stimulant results in the plant

converting chemical energy into forces that cause tissue deformation and movement [3].

Synthetic nastic structures are modeled after motor cells and the biochemistry that drives them. Nastic structures are composed of a polymer embedded with an array of hydraulic microactuators that are driven by energy released by ATP hydrolysis and used by active transport. The actuator housing plate polymer is designed to be flexible enough to allow controlled deformation while in the process of actuation, yet rigid enough to withstand outside forces without material fracture or failure. The range of actuation is controlled by the level of biochemical energy in the process. Energy variation across the plane of actuators will result in non-uniform actuation, causing local expansion and overall bending or twisting. As in plants, differing material displacement will cause motion and shape change.

Nastic structures are desirable for use in mechanical systems that employ morphing parts that must sustain high levels of stress (Figure 1). An example of nastic structures application is in the field of inflating and morphing wings for aerial vehicles. For nastic structures to be efficient and safely used in mechanical applications, a number of qualities are required that are considered in their research and design. Some requirements of nastic actuator systems include a low power consumption, rapid reaction speed, low weight, high blocked stress, ability to be actuated repeatedly with little residual stress and fatigue, and the capability to sustain a deflected position over time and under stress [4].

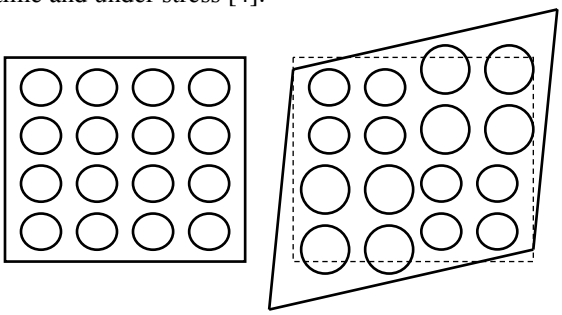

Figure 1: Nastic actuator arrays, before and after local actuation causes expansion and twisting shape change

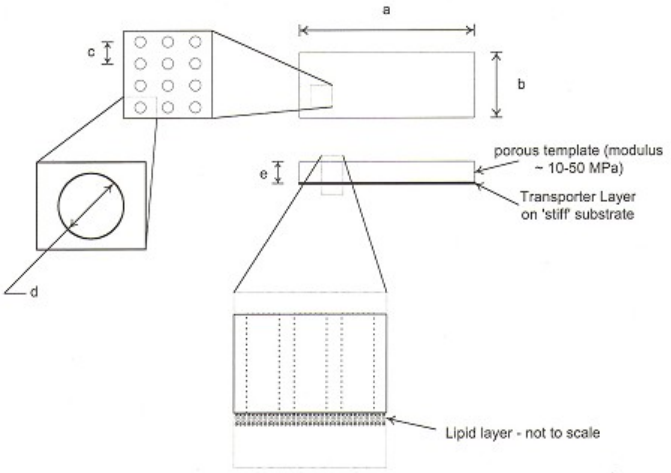

Figure 2: Micro-hydraulic actuation plate for nastic structures experiments

CONSTRUCTION AND PHYSCIAL PROPERTIES OF NASTIC STRUCTURES

The essential components of the nastic actuator are a reservoir, a membrane with biological transporters and a deformable chamber into which fluid can be pumped in, to result in planar or volumetric strain. The schematic of a nastic actuator that exhibits planar strain on the cover plate was discussed in ref. [2]; its current version is shown in Figure 2.

The micro hydraulic actuator plate is 1 mm thick and has an array of through holes 0.8 mm to 1.0 mm in diameter. Each hole in the micro-hydraulic actuator plate is referred to as a 'barrel'. Walls of the barrel chamber are assumed to exhibit negligible strain as fluid pressure increases inside. The membrane assembly is a Polypropylene glycol – Diacrylate membrane which supports the lipid bilayer dispersed with transporters and is considered to be rigid for analysis, as membrane deformation is assumed to be small enough to not have any significant impact on volume change during actuation, since the membrane is between two fluids with high osmotic pressure. The cover plate is the only deformable material with elastic modulus in the range 0.1 GPa to 2 GPa. The actuator parameters will be varied to achieve the desired strain on the cover plate.

BIOCHEMICAL ENERGY SYSTEMS OF SYNTHETIC NASTIC ACTUATORS

Energy Released by ATP Hydrolysis

Various metabolic pathways break down carbohydrates such as glucose to release energy and ATP. ATP is assembled by the joining of ADP and PO_4^{2-} with a phosphoanhydride bond. When this bond is broken, energy is released. The amount of free energy released depends on the concentration of reactant ATP and its products, and the hydrogen ion concentration. The concentration of reactant and products are evaluated as the mass-action ration, K_{ma}, and the hydrogen concentration is evaluated as pH. All concentrations are in moles per liter. The reaction takes place in an aqueous solution, but water concentration is evaluated at unity, not reacting in the equation.

$$ATP + H_2O \rightarrow ADP + PO_4^{2-} + \Delta G_{atph} \quad (1)$$

$$K_{ma} = \frac{[ATP]}{[ADP][PO_4^{2-}]} \quad (2)$$

$$pH = -\log[H^+] \quad (3)$$

The free energy of ATP hydrolysis under standard temperature, concentration, and pH is -30.5 kJ/mol, expressed as ΔG^0. However, the concentrations will vary as a means of controlling actuation by inhibiting energy release to limit the range of active transport. Variation in pH is another means of energy control. Therefore an equation to show the energy released by ATP hydrolysis, ΔG, is required.

Evaluating the effects of pH variation involves a simple adjustment of the standard free energy. Also, the effects of a

temperature change can be noted. However, the temperature is commonly analyzed as a constant, 300 K and so has no influence on the system, as it would be an illogical and inconvenient way to control an actuation system. However, as nastic structures are considered for use in aerospace application, where temperature can rapidly change, the effect of temperatue on nastic structures as well as actuator response to counter averse temperature changes will be analyzed in future study. R is the universal gas constant, expressed as L*kPa/mol*K. The energy released is in kJ/mol.

$$\Delta G_{pH} = \Delta G^0 - RT(pH) \tag{4}$$

Because pH is the negative logarithm of molar hydrogen ion concentration, variation in hydrogen in the ATP solution causes an exponential change in energy release. Further incorporation of a variable mass-action ratio is similarly evaluated. As the hydrogen ions concentration is evaluated as a logarithm, so it the mass-action ratio.

$$\Delta \mathrm{G} = \Delta \mathrm{G}^0 - R*T*\mathrm{pH} + R*T(\ln(\mathrm{K_{ma}}) + \mathrm{pH}) \tag{5}$$

Simplified, the equation for energy released by ATP hydrolysis under variable pH and mass-action ratio is:

$$\Delta \mathrm{G} = -30.5 - R*T(\ln(\mathrm{K_{ma}}) + 2\mathrm{pH}) \tag{6}$$

The overall value for ΔG will always be negative because energy is released in the reaction. It is feasible to control the amount of energy released by directly changing the concentration levels of ATP and hydrogen ions. By raising or lowering the molar concentration, the amount of energy released can be accurately modified, limiting the energy available for active transport usage.

Energy Required for Fluid Flux Through Active Transport

Active transport proteins require energy to transfer water molecules from a low-concentration area to a high-concentration area. The greater the difference in concentrations, the more energy is required. The chamber of the nastic actuator expands due to fluid pressure causing outward volumetric deflection, and so active transport proteins will require an increasing amount of energy as the fluid concentration inside the actuator increases. A constant energy input will not be sufficient to power active transport. To determine the minimum amount of energy required to move water from a reservoir into the actuator chamber, the membrane transport system must be analyzed to ensure that ATP hydrolysis conditions are sufficient to power actuation.

The energy change in kJ/mol for the movement of an uncharged particle from one side of a membrane at concentration C1 to the other side at a higher concentration C1, and solute concentration K_{eq}, is given [6] by:

$$\Delta E = -R*T\ln K_{eq} + R*T\ln\frac{C2}{C1} \tag{7}$$

Since the solute considered in this case is water, its concentration can be evaluated as unity, simplifying the equation to:

$$\Delta E = R*T\ln\frac{C2}{C1} \tag{8}$$

Concentration is in moles per liter, but in calculating the material deflection due to fluid force, pressure is in MPa. Fluid compression and bulk modulus will be addressed later in this paper, but for biochemical purposes, the pressure and concentration have a linear relationship and compressibility and bulk modulus do not have any part in active transport energy use. To convert osmotic pressure in MPa, to molar concentration in Mol/L, the following well-known equation is used to ensure dimensional balance:

$$C_{mol} = \frac{P}{R*T} \tag{9}$$

As the system actuates, the fluid concentration inside the actuator, C2, increases steadily. It is assumed that the concentration outside the membrane, C1, will remain constant as water is moved into the fluid reservoir to replenish the water that moved from the fluid reservoir into the actuator chamber. Because of this, C2/C1 is a linear ratio. Equation (8) becomes:

$$\Delta E = R*T\ln C_R \tag{10}$$

C_R is the ratio of fluid concentration in the actuator chamber to the concentration in the fluid reservoir outside the membrane. As the osmotic pressure inside the actuator increases, the energy required to continue actuation by sustaining the active transport of water into an ever increasing concentration will rise exponentially. However, since it was shown earlier that change in mass-action ratio and pH will cause ATP hydrolysis to release more energy at an exponential rate, ATP hydrolysis is a feasible energy source for active transport to power nastic actuation.

Control Mechanisms for Active Transport

ATP hydrolysis conditions can be modified to control the range of actuation by inhibiting energy release. Likewise, the membrane active transport proteins are affected by the material and solute properties. Modifying these properties can similarly limit the amount of fluid transferred across the membrane, becoming a potential source of actuation control.

Calcium and sodium in cells in conjunction with the enzyme ATPase has been observed to affect the active transport process [6]. It is possible for the membrane proteins in nastic structure membranes to imitate cells that have Na-mediated ion protein pumps. In such cells, Ca inhibits the reaction on Na and the transport proteins. By increasing the concentration of Ca in the fluid reservoir, the amount of fluid transported would decrease due to interaction with Na, preventing the activation of protein transport [7]. To increase the amount of transport activity after inhibition, Na could be introduced to the medium while Ca is removed through chemical means. There are other metabolic inhibitors, such as cyanide and fluoracetate that

suppress active transport in animal cells [8] but it is not yet known if the inhibitory effect would be reversible in a synthetic system, and may not be plausible for actuator use.

In some animal cells, an electrical charge is created in the membrane during active transport when ion movement is promoted by the enzyme ATPase. Investigation of using an electrical charge on the membrane as a source of flux control is plausible. During transport, ATPase will cause the movement of Na+ ions out of the membrane while moving K+ ions inward with the fluid. Because of the resulting Na+/K+ concentration ratio, an electrical gradient is formed in the membrane. When the membrane and substrate passing through it are charged, the energy required for active transport is:

$$\Delta E = R*T*\ln(C_R) + ZF\Delta\Psi \qquad (11)$$

In this equation, Z is the net charge on the transported molecule, F is Faraday's constant, and $\Delta\Psi$ is the membrane voltage. Sodium or potassium could be easily added or removed from the ATP solution to raise or lower the energy required for active transport, thereby inhibiting the volume flow allowed by the membrane proteins and limiting the range of hydraulic actuation.

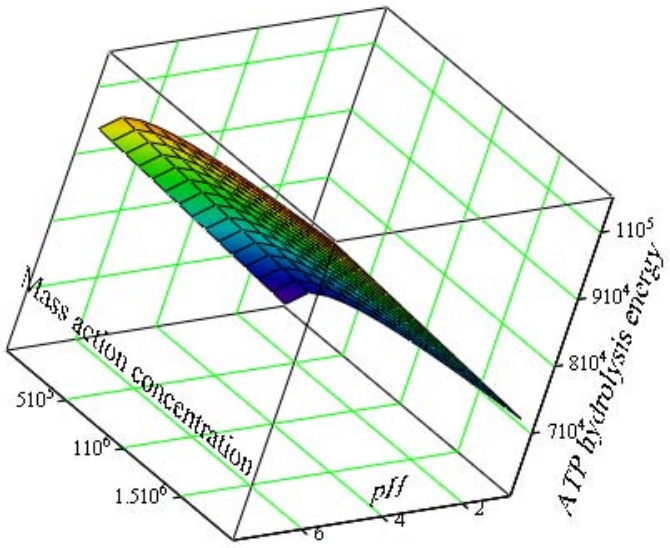

Figure 3: Effect of pH and mass action concentration on ATP hydrolysis energy release

MODELING OF MECHANICAL NASTIC ACTUATION

We will start the analysis with a simple mechanical model of an actuating nastic structure (Figure 2). Consider a perforated plate with a regular pattern on circular holes. At the bottom of plate, we have a membrane transferring fluid through nastic action into each hole and creating nastic pressure. At the top of the plate, we have an elastic membrane that will deform under the action of the nastic pressure thus creating actuation. For our model, we will consider a unit cell cut out from the plate (Figure 4).

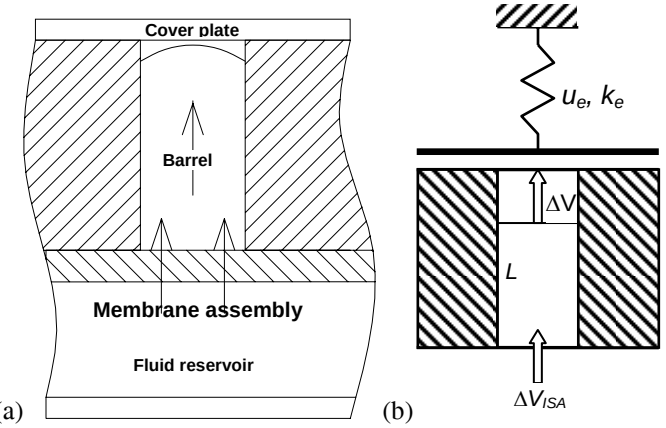

Figure 4: Unit-cell in the actuator plate: (a) functional schematic; (b) modeling schematic

The input in is dissipated into several compliance mechanisms: fluid compressibility, barrel expansion, cap bulging under internal pressure and under external load. Displacement analysis is performed by summing the volume changes associated with each compliance mechanism:

$$\Delta V_{ISA} = \Delta V_{comp} + \Delta V_{barrel} + \Delta V_{cap}^{pressure} - \Delta V_{cap}^{Load} \qquad (12)$$

The energy analysis is performed by summing the energy changes associated with each compliance mechanism:

$$p\cdot\Delta V_{ISA} = p\cdot\Delta V_{comp} + p\cdot\Delta V_{barrel} + p\cdot\Delta V_{cap}^{pressure} + P\cdot\Delta u_e \qquad (13)$$

where $p\cdot\Delta V$ is the incremental energy input, $P\cdot\Delta u_e$ is the incremental external work, and the rest is the incremental energy expended internally do the structural compliance.

Material Dimensions and Properties

Table 1 shows the variables considered in the mechanical analysis of nastic actuation. These variables are considered *master variables*. Other variables are also considered, but as dependent variables. For example, the internal diameter of the barrel, *d*, is a master variable, whereas the internal radius, $r_f = d/2$ is a dependent variable. Similarly, the hole pitch and external radius of the barrel, r_s, is also a dependent variable that depends on the diameter *d* and on the percentage pitch, *%d*, in the form

$$pitch(d,\%d) = d\cdot\%d \qquad (14)$$

$$r_s(d,\%d) = \frac{1}{2}pitch(d,\%d) \qquad (15)$$

The analysis aims at expressing everything in terms of the master variables through multivariable analytical functions. This permits the performing of multivariable parametric analysis with the aim of determining the optimal nastic structure configuration.

Table 1: Master variables considered in the mechanical modeling

Symbol	Description	Default value	Min value	Max value
d	Barrel diameter	200 micron	50 micron	1000 micron
%d	% pitch	150%	130%	400%
h	Barrel height	200 micron	100 micron	400 micron
t	Cap thickness	20 micron	10 micron	60 micron
E	Modulus of elasticity	2 GPa	2 GPa	30 GPa
ν	Poisson ratio	0.45	0.45	0.45
B	Fluid compressibility	2.2 GPa	2.2 GPa	2.2 GPa
p	Pressure	5 MPa	0 MPa	5 MPa
P	Point load	0 mN	0 mN	39.3 mN

Fluid compressibility

The volume increment due to fluid compressibility is

$$\Delta V_F(d,h,B,p) = \frac{p}{B}V(d,h)\,, \quad V(d,h) = \pi r_f^2(d)h \tag{16}$$

where B is the fluid bulk modulus. Equation (16) shows that the volume change due to fluid compressibility is a function of diameter, *d,* height, *h,* fluid modulus, *B*, and pressure, *p*. The expression ΔV_B given by Equation (20) represents the contribution ΔV_{comp} of Equation (12).

Barrel compressibility

Barrel compressibility yields the following volume increment

$$\Delta V_B = 2\pi r_f \cdot u_R \cdot u_L \tag{17}$$

where u_L the longitudinal displacement (expansion) of the barrel and u_R is the radial displacement (expansion) of the barrel. The longitudinal displacement is calculated the height-wise expansion under the fluid pressure acting at the cylinder ends, i.e.,

$$u_L = \frac{r_s^2}{r_s^2 - r_f^2}\frac{p}{E}h \tag{18}$$

The radial expansion is calculated using the analytical solution for thick-wall cylinders[9], i.e.,

$$u_R = \frac{r_f\left[(1+\nu)r_s^2 + (1-\nu)r_f^2\right]}{r_s^2 - r_f^2}\frac{p}{E} \tag{19}$$

Since r_f is function of *d*, i.e., $r_f = r_f(d)$ and since r_s is function of *d* and *%d*, it follows from Equations (18) and (19) that the displacements u_L and u_R are function of *d, %d, E,* and *p*, i.e., $u_L = u_L(d,\%d,h,E,p)$ and $u_R = u_R(d,\%d,E,p)$. Substitution in Equation (17) yields the volume increment due to barrel compressibility as a function of *d, %d, h, E,* and *p*, i.e., $\Delta V_B = \Delta V_B(d,\%d,h,E,p)$, i.e.,

$$\Delta V_B(d,\%d,h,E,p) = 2\pi \cdot r_f(d) \cdot u_L(d,\%d,h,E,p) \cdot u_R(d,\%d,E,p) \tag{20}$$

The expression ΔV_B given by Equation (20) represents the contribution ΔV_{barrel} of Equation (12).

Outwards bulging of the cap under internal pressure

To calculate the volume increment due to the cap bulging under internal pressure, we consider the plate-bending analytical solution [9] that gives the radial variation of the plate displacement in the form

$$u_C(r) = \frac{pr_f^4}{64 f_g}\left(1-r^2\right)^2 \tag{21}$$

The subscript "C" stands for "clamped", and signifies that clamped boundary conditions around the plate boundary have been assumed. The symbol f_g is the plate bending stiffness given by

$$f_g = \frac{1}{12\left(1-\nu^2\right)}Et^3 \tag{22}$$

The central deflection of the cap under internal pressure is

$$u_{C\max} = \frac{p \cdot r_f^4}{64 f_g} \tag{23}$$

The volume increment due to cap bulging is calculated by integration of Equation (21), i.e.,

$$\Delta V_C = \int_0^{r_f} u_C(r)\left[2\pi r\right]dr = \frac{\pi}{3}\cdot\frac{7+\nu}{1+\nu}\frac{p \cdot r_f^6}{64 f_g} \tag{24}$$

Since r_f is function of *d*, i.e., $r_f = r_f(d)$, and since f_g is function of E and t, i.e., $f_g = f_g(E,t)$, it follows from Equation (23) and (24) that the displacement $u_{C\max}$ and the volume increment due to plate bulging are function of *d, E, t,* and *p*, i.e., $u_{C\max} = u_{C\max}(d,E,t,p)$ and $\Delta V_C = \Delta V_C(d,E,t,p)$. Substitution in Equation (24) yields the volume increment due to cap bulging as a function

$$u_{C\max}(d,E,t,p) = \frac{p \cdot r_f^4(d)}{64 f_g(E,t)} \tag{25}$$

$$\Delta V_C(d,E,t,p) = \frac{\pi}{3}\cdot\frac{p \cdot r_f^6(d)}{64 f_g(E,t)} \tag{26}$$

The expression ΔV_C given by Equation (26) represents the contribution $\Delta V_{cap}^{pressure}$ of Equation (12).

Inwards bulging of the cap under external load

To calculate the volume increment due to the cap bulging inwards under external load, we consider the plate-bending analytical solution [9] that gives the radial variation of the plate displacement in the form

$$u_{CP}(r) = \begin{cases} \dfrac{Pr_f^2}{64\pi f_g}\left(2r^2\ln r - r^2 + 1\right) & \text{if } r \neq 0 \\ \dfrac{Pr_f^2}{16\pi f_g} & \text{if } r \neq 0 \end{cases} \tag{27}$$

The subscript "CP" stands for "clamped *P*", and signifies that clamped boundary conditions and central point force *P* have been assumed. The central deflection of the cap under internal pressure is

$$u_{CP\max} = \frac{P \cdot r_f^2}{16\pi f_g} \tag{28}$$

The volume increment due to cap bulging is calculated by integration of Equation (21), i.e.,

$$\Delta V_{CP} = \int_0^{r_f} u_{CP}(r)\left[2\pi r\right]dr = \frac{Pr_f^4}{64 f_g} \tag{29}$$

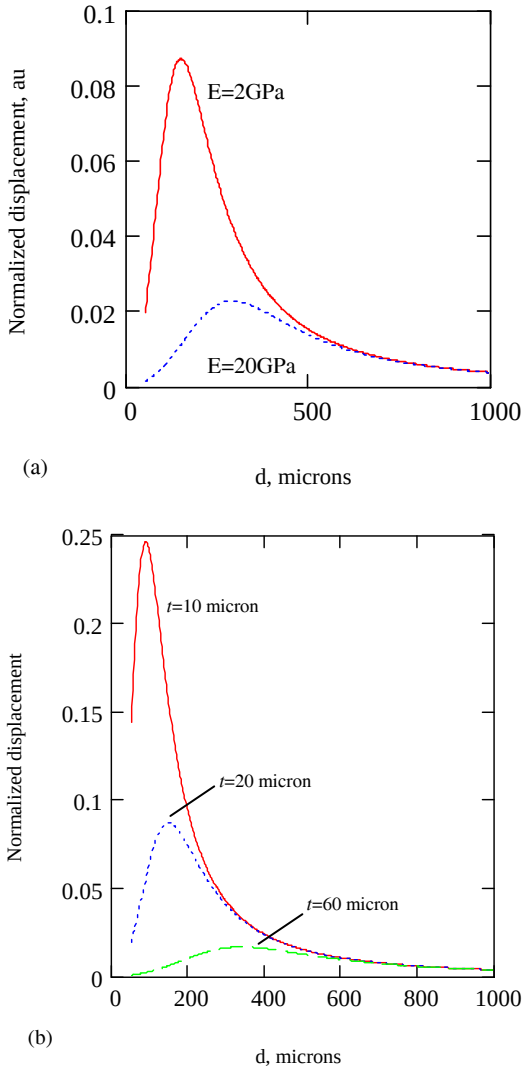

Figure 5: Actuation displacement normalized to actuation volume as function of barrel diameter: (a) dependence on modulus, *E*; (b) dependence on cap thickness, *t* (plate height is set to the default value h_0=200 micron)

Since r_f is function of d, i.e., $r_f = r_f(d)$, and since f_g is function of E and t, i.e., $f_g = f_g(E,t)$, it follows from Equations (27) and (29) that the central displacement and the volume increment due to plate bulging under external point load are function of d, E, t, and P, i.e., $u_{CP\max} = u_{CP\max}(d,E,t,P)$ and $\Delta V_{CP} = \Delta V_{CP}(d,E,t,P)$. Substitution in Equation (24) yields the volume increment due to cap bulging as a function

$$u_{CP\max}(d,E,t,p) = \frac{P\cdot r_f^2(d)}{16\pi f_g(E,t)} \tag{30}$$

$$\Delta V_{CP}(d,E,t,P) = \frac{P\cdot r_f^4(d)}{64 f_g(E,t)} \tag{31}$$

The expression ΔV_{CP} given by Equation (20) represents the contribution ΔV_{cap}^{Load} of Equation (12).

Plate stiffness and blocked force

We can also calculate the stiffness of the plate under external point load, k_{CP}, by dividing the central deflection by the applied force. Hence,

$$k_{CP}(d,E,t) = \frac{4\pi Et^3}{(1-\nu^2)r_f^2(d)} \tag{32}$$

The blocked force is calculated as the external load that will compensate for the outwards bulging of the plate thus making the central deflection zero. Combining Equations (23) and (28) yields the blocked force expression as

$$P_{bk}(d,p) = \frac{\pi p\cdot r_f^2(d)}{4} \tag{33}$$

Total volumetric displacement

Adding together the various contributions outlined above yields the total volumetric displacement as

$$\begin{aligned}\Delta V(d,\%d,h,B,E,t,p,P) = {} & \Delta V_F(d,h,B,p) \\ & +\Delta V_B(d,\%d,h,E,p) \\ & +\Delta V_C(d,E,t,p) \\ & -\Delta V_{CP}(d,E,t,P)\end{aligned} \tag{34}$$

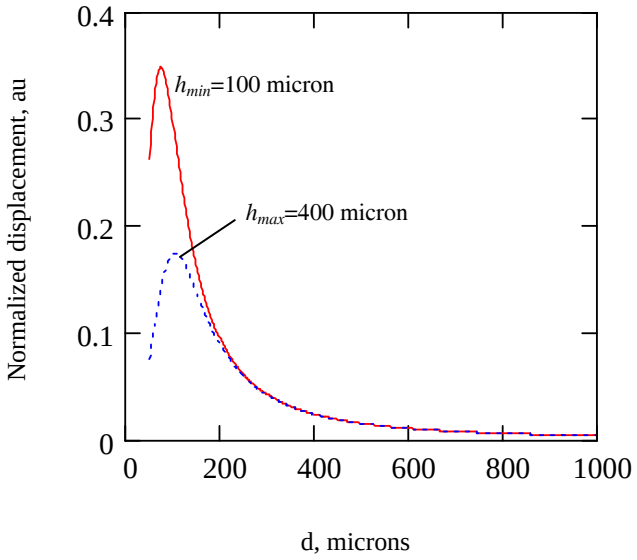

Figure 6: Actuation displacement normalized to actuation volume as function of barrel diameter showing dependence on plate height, *h* (modulus and cap thickness are kept at minimum values, E_{min}=2GPa, t_{min}=10 micron)

DISCUSSION

The volumetric displacement described by Equation (34) is essential in estimating the actuation efficiency. It indicates how much volume must be pumped through the nastic process in order to achieve a certain actuation displacement on the nastic plate top. Since the volumetric displacement depends on eight parameters (*d, %d, h, B, E, t, p, P*), this dependence relation is rather intricate. In our study, we found of interest to investigate

the optimum actuation displacement, i.e., we studied the displacement normalized with respect to the actuation volume. The aim was to find optimum values of the design variables that would give the maximum actuation displacement for a given actuation volume. Thus, the normalized actuation displacement was plotted vs. the barrel diameter, *d*, with the aim of finding the diameter values that would produce peaks of the normalized actuation displacement. The results are shown in Figure 5 and Figure 6. It can be seen from these figures that peak values of the normalized displacement is obtained at barrel diameters between 100 and 400 microns. However, the location and amplitude of these peaks strongly depends on the values of other parameters. In our study, three parameters were considered: (a) elastic modulus, *E*; (b) cap thickness, *t*; and (c) plate height, *h*. It was found that an increase in elastic modulus reduces the peak amplitude and shifts its location to higher *d* values (Figure 5a). The influence of cap thickness, *t*, is in the same direction, i.e., an increase in cap thickness results in a lower peak shifted to the higher *d* values (Figure 5b). Similarly, the increase in plate height, *h*, also results in a decrease in normalized actuation displacement, but with very little shift in peak location.

CONCLUSIONS

Physical properties that affect the range of deflection work done by nastic actuation were examined, in addition to discussion of the biochemical reactions found in nastic plant movement that are to be imitated synthetically to power actuation. Several means of controlling physical actuation by modifying chemical properties were discussed. By using a pH gradient in the ATP solution, the amount of energy released in ATP hydrolysis can be inhibited, controlling the available energy for use in powering active transport. Limiting this energy puts a ceiling on the volume of water that can be transported, thereby controlling the change in osmotic pressure within the actuator that causes the outward forces of deflection. A mechanical model of the actuation mechanism was developed. The model depends on eight design parameters (*d, %d, h, B, E, t, p, P*). Parameter studies were conducted to determine optimum conditions in which maximum actuation displacement is obtained for a given nastic actuation volume. These preliminary results have the potential to be used in the design and construction of optimum nastic actuation specimens. Further optimization studies will be carried out to determine the influence of the design parameters on the nastic structure power and energy capabilities.

NOMENCLATURE

B= Fluid bulk modulus

C_r= Ratio of fluid concentrations in the actuation cylinder and fluid reservoir, dimensionless

D= Barrel diameter, microns

%d= Pitch, distance between actuator barrels as a percentage of d

E= Modulus of Elasticity, GPa

ΔE= Energy used by active transport, kJ/mol

f_G= Plate bending stiffness

ΔG=Energy released by ATP Hydrolysis, kJ/mol

h= Barrel height, microns

K_{cp}= Plate stiffness under external load

K_{ma}= Mass-action balance, ratio of reactant to products in ATP hydrolysis, dimensionless

ν= Poisson's ratio

P= Point load, mN

P_a= Osmotic pressure of actuation cylinder, kPa

P_{bk}= Blocked force

P_f= Osmotic pressure of fluid reservoir, kPa

pH=pH level of ATP solution, -log[H+ concentration, mol/L]

R= 8.31447 L*kPa/mol*K

T= temperature of the environment, K

t= Cover plate/cap thickness, microns

u_C= Cap displacement, microns

u_L= Barrel longitudinal displacement, microns

u_R= Barrel radial expansion, microns

ΔV_B= Volume change due to barrel compressibility, pL

ΔV_C= Volume change due to cap displacement, pL

ΔV_F= Volume change due to fluid compressibility, pL

ΔV_{ISA}= Total volume change, pL

ACKNOWLEDGMENTS

The financial support of DARPA, Dr. John Main program manager is thankfully acknowledged.

REFERENCES

[1] Forterre, Y., Skotheim, J.M., Dumais J. & Mahadevan, L. (2005) How the Venus Flytrap Snaps. *Nature*, 433: 421-425, 2005

[2] Hope, A.B. (1971) Ion Transport and Membranes- A Biophysical Outline. University Park Press, Baltimore, 1971

[3] Leo, D., Sundaresan, V.B., Tan, H., Cuppoletti, J. (2004) Investigation on High Energy Density Materials Utilizing Biological Transport Mechanisms.ASME-IMECE2005-60714, 2004

[4] Cadogan, D., Smith, T., Uhelsky, F., MacKusick, M. (2005) Morphing Inflatable Wing Development for Compact Package Unmanned Aerial Vehicles. *American Institute of Aeronautics and Astronautics- Adaptive Structures Forum,* 2004

[5] Nelson. D., Cox, M. (2000) Lehninger Principles of Biochemistry. Worth Publishers, 2000

[6] Segel, I. (1976) Biochemical Calculations- How to Solve Mathematical Problems in Biochemistry. John Wiley & Sons, Inc., 1976.

[7] Brown, A., Lew, V. (1983) Inhibition of the Na Pump by Cytoplasmic Calcium in Intact Blood Cells, *Current Topics in Membranes and Transport*, 19: 1017-1023, 1983

[8] Quastel, J.H. (1960) Transport at Cell Membranes and Regulation of Cell Metabolism. *Membrane Transport and Metabolism, Czechoslovak Academy of Sciences*, 1960

[9] Massonnet, Cg. (1962) "Two Dimensional Problems", Chapter 37 in *Handbook of Engineering Mechanics*, W. Flugge (Ed.), McGraw-Hill, 1962

[10] Way, S. (1962) "Plates" Chapter 39 in *Handbook of Engineering Mechanics*, W. Flugge (Ed.), McGraw-Hill, NY, 1962